

# PHOTOCATALYTIC DECOMPOSITION OF ISOLAN BLACK BY $\text{TiO}_2$ , $\text{TiO}_2$ - $\text{SiO}_2$ CORE SHELL NANOCOMPOSITES

K. Balachandran<sup>1</sup>, R. Venckatesh<sup>2</sup>, Rajeshwari Sivaraj<sup>3</sup>

<sup>1</sup>Department. of Chemistry, Vivekanandha College of Engineering for Women, Tiruchengode-637 205, Tamilnadu, India,

<sup>2</sup>Department of Chemistry, Government Arts College, Udumalpet, Tamilnadu, India

<sup>3</sup>Department of Biotechnology, Karpagam University, Coimbatore, Tamilnadu, India,

balanano06@gmail.com, rvenckat@gmail.com, rajs@gmail.com

Corresponding Author: K. Balachandran

## Abstract

Anatase phase  $\text{TiO}_2$ ,  $\text{TiO}_2$ - $\text{SiO}_2$  (TS) photocatalyst were prepared by wet chemical technique. The synthesized nano particles were characterized by XRD, SEM-EDAX, TEM, UV and FTIR spectroscopy. The grain size of the  $\text{TiO}_2$  nanoparticles was found to be 24nm, while 7-10nm for  $\text{TiO}_2$ - $\text{SiO}_2$  was calculated by using Scherrer's formula. The  $\text{TiO}_2$ - $\text{SiO}_2$  core shell nanocomposites were identified by TEM analysis. Ti-O, Si-O bonds were confirmed by EDAX and FTIR. The photocatalytic decomposition of Isolan black was investigated. The photocatalytic activity of  $\text{TiO}_2$ , enhanced by doping of  $\text{SiO}_2$  on  $\text{TiO}_2$ . The important factors such as pH, Wt % of dyes and nanoparticles, intensity of light are also affect the photocatalytic action.

**Index Terms:** Nanocomposites, Photocatalyst, TEM, SEM-EDAX.

\*\*\*

## 1. INTRODUCTION

The waste water that is characterized with high colour, high COD, low biodegradability and high variability has seriously polluted the drain water. Among the problems it causes colour. The most critical dye stuff is the primary source of colour. Most of the dye stuffs are complicated aromatic compounds and are chemically stable. Through the waste water posses the low BOD/COD ratio, colour, COD and residual dye level are still high even after traditional biological treatment or chemical coagulation treatment. Without further treatment the waste water will not meet the ever stricter environmental standards of discharged water.

Many processes have been proposed over the years and are currently used to remove organic toxins from waste water. Current treatment methods for these contaminants such as adsorption by activated carbon and air stripping, merely concentrate the chemicals present by transferring them to the adsorbent or air, but they do not convert them into non toxic wastes. Thus one of the major advantages of the photocatalytic process over existing technologies is that there is no further requirement for secondary disposal methods [1].

During the photocatalytic process, the illumination of a semiconductor photocatalyst with ultraviolet radiation activates the catalyst, establishing a redox environment in the aqueous solution [2]. Semiconductors act as sensitizers for light induced redox process due to their electronic structure, which is characterized by a filled valence band and an empty

conduction band [3]. The energy difference between the valence band and conduction band is called bandgap. Nanocrystalline photocatalysts are ultra small semiconductor particles which are few nanometers in size. During the past decade, the photochemistry of nano semiconductor particles originates from their unique photophysical and photocatalytic properties [4]. Due to their large surface area, nano sized catalyst particles show a significantly enhanced reactivity compared to larger particles or bulk material.

Heterogeneous photocatalysis a promising technology in environmental cleanup is mostly based on the semiconductor photocatalyst nanocrystalline  $\text{TiO}_2$  [5], because it is nontoxic, easy to be made, inexpensive and chemically stable [6-8]. Photooxidation by using  $\text{TiO}_2$  photocatalyst is being widely studied as a relatively new technique of pollution abatement.  $\text{TiO}_2$  is a commonly used photocatalyst because of its stability in UV light and water [9].

Furthermore to improve the efficiency of the catalytic activity more emphasis is placed on mixing  $\text{TiO}_2$  with  $\text{SiO}_2$  [10]. The addition of  $\text{SiO}_2$  helps to create new catalytic active sites due to interaction between  $\text{TiO}_2$  and  $\text{SiO}_2$  [10-13]. By introducing  $\text{SiO}_2$  on  $\text{TiO}_2$  can transform amorphous phase to crystalline anatase phase [14]. Titania-Silica mixed oxides have a large number of applications in catalysis either as catalyst by themselves or as catalyst support [15].  $\text{TiO}_2$ - $\text{SiO}_2$  mixed oxides shows a higher thermal stability, adsorption capability and good redox properties [16]. A number of methods have been applied to prepare  $\text{TiO}_2$ - $\text{SiO}_2$  composites, including e

beam evaporation, chemical vapor deposition flame hydrolysis and sol-gel method. Among all type of synthesis methods Solgel method has several advantages good homogeneity, ease of composition control, low processing temperature, ability to fabricate large area coatings and low equipment cost [17]. The size and shapes are also modified by Solgel techniques. This technique can be employed for development of optical coatings and wave guides [18].

In this present work we synthesis  $\text{TiO}_2$ ,  $\text{TiO}_2$ - $\text{SiO}_2$  core shell nanocomposites by Solgel method at room temperature. The composite was analyzed for grain size by XRD, surface morphology and composition by SEM-EDAX, band gap by UV-visible spectra, metal oxide bonds by FT-IR spectra and the photocatalytic decomposition studies of Isolan black was investigated by UV-Visible spectroscopy.

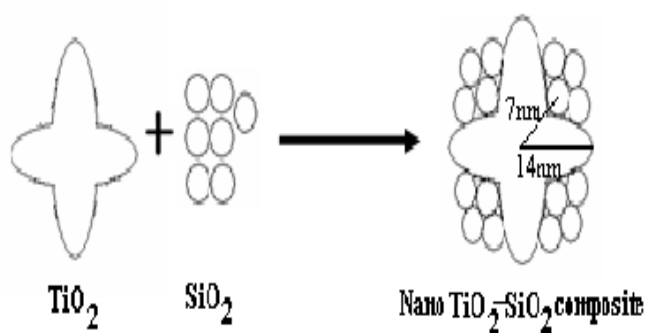
## 2. EXPERIMENTAL

### 2.1. MATERIALS

All reagents used were of analytical grade purity and were procured from Merck Chemical Reagent Co. Ltd. India.

### 2.2 PREPARATION OF NANOCOMPOSITES

In the synthesis of  $\text{TiO}_2$  particles, Titanium tetra isopropoxide was used as a precursor and it was mixed with HCl, ethanol and deionised water mixture, stirred for half an hour, in pH range of 1.5. 10 ml of deionised water was added to the above mixture and stirred for 2 hours at room temperature. Finally the solution was dried at room temperature and the powder was heated at  $120^\circ\text{C}$  for 1 hour. Silica particles were prepared from silicic acid and were stirred with THF for 1 hour. Then Titania gel was slowly added to the silica particles. The mixture was stirred for 3 hours and dried at room temperature. Finally the mixture was heated at  $120^\circ\text{C}$  for 1 hour.



### 2.3 CHARACTERIZATION

The prepared Nano particles were characterized for the crystalline structure using D8 Advance X-ray diffraction meter (Bruker AXS, Germany) at room temperature, operating at 30 kV and 30 mA, using  $\text{CuK}\alpha$  radiation ( $\lambda = 0.15406 \text{ nm}$ ). The

crystal size was calculated by Scherrer's formula. Surface morphology was studied by using SEM-EDS (Model JSM 6390LV, JOEL, USA), UV-Vis diffuse reflectance spectra were recorded with a Carry 5000 UV-Vis-NIR spectrophotometer (Varian, USA) and FTIR spectra were measured on an AVATAR 370-IR spectrometer (Thermo Nicolet, USA) with a wave number range of  $4000$  to  $400 \text{ cm}^{-1}$ .

## 2.4 PHOTOCATALYTIC STUDIES

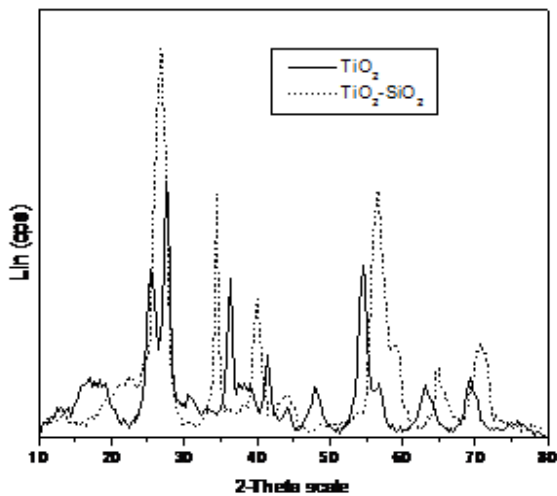
Photocatalytic activity of the as-prepared particles for the environmental application was evaluated by measuring the photo degradation of methylene blue (MB) in water under sunlight irradiation. The initial concentration of MB was  $50 \text{ mg l}^{-1}$  and the concentration of nanoparticles was  $1.0 \text{ g l}^{-1}$ .

## 3. RESULT AND DISCUSSION

Fig.1 shows the XRD patterns of sol-gel derived  $\text{TiO}_2$  and nano  $\text{TiO}_2$ - $\text{SiO}_2$  composites. The crystallite type of the TS nano composite particles was the pure anatase. The most intense reflection at  $2\theta = 25.3^\circ$  is assigned to anatase (d101). Not much difference has been detected between patterns of  $\text{TiO}_2$  and  $\text{TiO}_2$ - $\text{SiO}_2$ . The powders showed the crystalline pattern and the observed d-lines match the reported values for the anatase phase. The intensity of reflections appeared to be decreased for  $\text{TiO}_2$ - $\text{SiO}_2$  as compared to  $\text{TiO}_2$  due to inclusion of amorphous  $\text{SiO}_2$ . The average crystallite size was determined by carrying slow scan of the powders in the range  $24$ – $27^\circ$  with the step of  $0.01^\circ$  from the Scherrer's equation using the (101) reflections of the anatase phase assuming spherical particles. An estimate of the grain size (G) from the broadening of the main (101) anatase peak can be done by using the Scherrer's formula

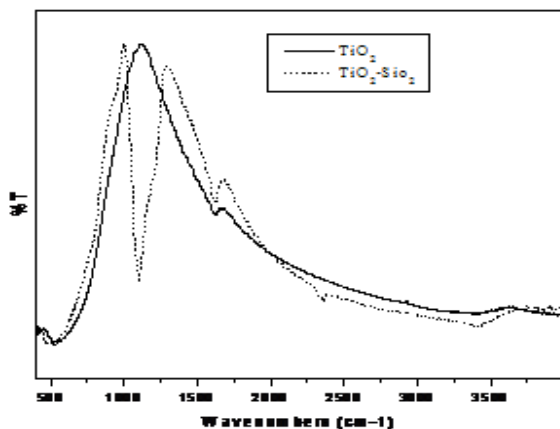
$$G = 0.9\lambda / \Delta(2\theta) \cos \theta \quad (1)$$

Where  $\lambda$  is the  $\text{Cu K}\alpha$  radiation wavelength and  $\Delta(2\theta)$  is peak width at half-height. The nanocrystallite sizes were found to be  $15$ – $20 \text{ nm}$  for  $\text{TiO}_2$  while  $7$ – $10 \text{ nm}$  for  $\text{TiO}_2$ - $\text{SiO}_2$  powders. The weakening and broadening of the XRD peaks may be attributed to the decrease of the sample grain size and the increase of the  $\text{SiO}_2$  content. The introduction of  $\text{SiO}_2$  can effectively suppress the grain growth of anatase compared with pure  $\text{TiO}_2$ . Moreover, the suppression is more remarkable with the introduction of higher silica content, which is consistent with the literature [19]. The major differences were the narrower first maximum and the broader second maximum.



**Fig1.** XRD patterns of  $\text{TiO}_2$ ,  $\text{TiO}_2\text{-SiO}_2$  nano composites.

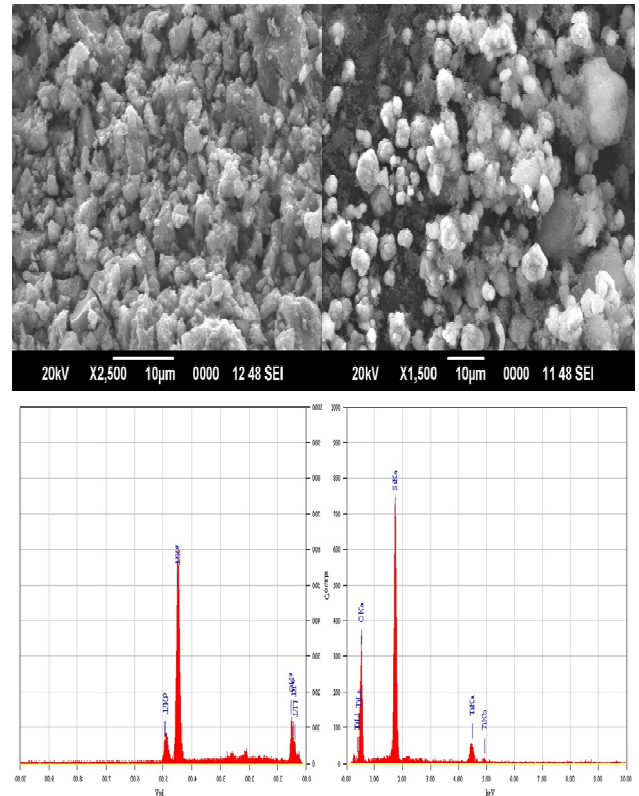
Fig.2 represents the FT-IR spectra of sol-gel derived  $\text{TiO}_2$ ,  $\text{TiO}_2\text{-SiO}_2$  composites. The peaks at  $3400$  and  $1650\text{ cm}^{-1}$  in the spectra are due to the stretching and bending vibration of the  $-\text{OH}$  group. In the spectrum of pure  $\text{TiO}_2$ , the peaks at  $550\text{ cm}^{-1}$  shows stretching vibration of  $\text{Ti-O}$  and peaks at  $1450\text{ cm}^{-1}$  show stretching vibrations of  $\text{Ti-O-Ti}$ . The spectrum of  $\text{TiO}_2\text{-SiO}_2$  show the peaks at  $1400\text{ cm}^{-1}$ ,  $450\text{-}550\text{ cm}^{-1}$  exhibiting stretching modes of  $\text{Ti-O-Ti}$ ,  $1100\text{ cm}^{-1}$  shows  $\text{Si-O-Si}$  bending vibrations and peak at  $950\text{ cm}^{-1}$  shows  $\text{Si-O-Ti}$  vibration modes which is due to the overlapping from vibrations of  $\text{Si-OH}$  and  $\text{Si-O-Ti}$  bonds. This result indicates that the TS nano particles were prepared by a combination of  $\text{TiO}_2$  with  $\text{SiO}_2$  nano particles [20].



**Fig2.** FTIR patterns of  $\text{TiO}_2$ ,  $\text{TiO}_2\text{-SiO}_2$  nano composites

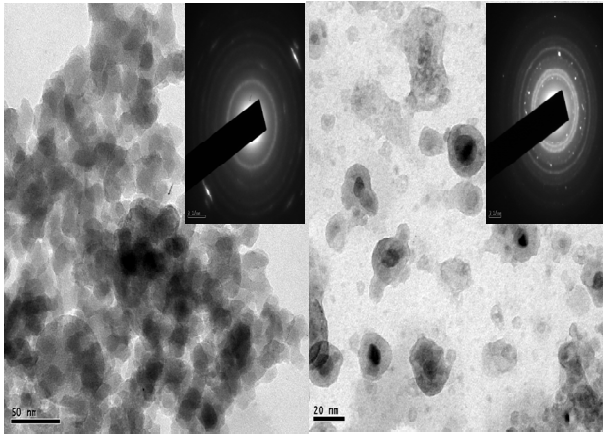
Fig.3 shows the SEM images along with the particle size distribution of the pure  $\text{TiO}_2$  sols and of the colloidal TS nano composites respectively. The pure  $\text{TiO}_2$  particles exhibited

irregular morphology due to the agglomeration of primary particles and with an average diameter of  $15\text{-}20\text{ nm}$ . On the other hand, the colloidal TS nanocomposites exhibited regular morphology, since the  $\text{TiO}_2$  cores were coated by  $\text{SiO}_2$  particles. The average particle size of the colloidal TS nano composites was measured to be  $7\text{-}10\text{ nm}$ . The EDAX analysis of  $\text{TiO}_2$ ,  $\text{TiO}_2\text{-SiO}_2$  nano composites confirms the presence of  $\text{Ti-O}$ ,  $\text{Si-O}$  bonds.



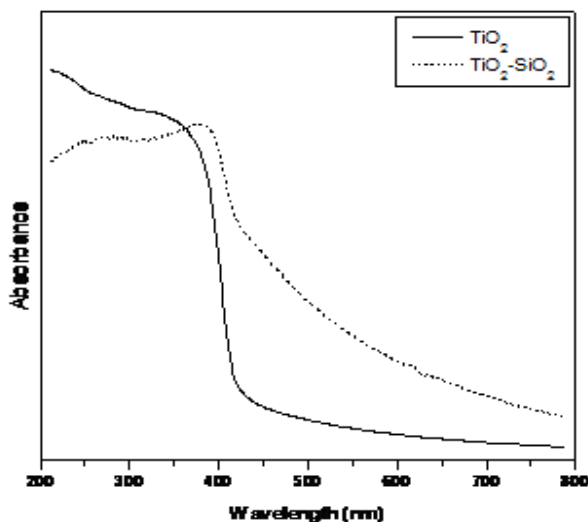
**Fig3:** SEM-EDAX analysis of  $\text{TiO}_2$ ,  $\text{TiO}_2\text{-SiO}_2$  nano composites.

Fig.4 represents the TEM images of  $\text{TiO}_2$  and nano  $\text{TiO}_2\text{-SiO}_2$  core shell nano composites. Transmission electron microscopic analysis strongly supported the nanophase formation of  $\text{TiO}_2$  and nano  $\text{TiO}_2\text{-SiO}_2$  core shell nano composites. The average particle size measured from TEM was found to be in the range of  $15\text{-}20\text{ nm}$  for  $\text{TiO}_2$ , and  $10\text{-}15\text{ nm}$  for TS, which was slightly varied from the particle size evaluated from diffraction method since in X-ray analysis it was assumed that the crystallites are formed without any local strain. From the TEM scale it was clearly observed that the particles exhibited in spherical in shape and in nanometer size. Fig 4b clearly shows the formation of  $\text{TiO}_2\text{-SiO}_2$  core shell nano composites.



**Fig.4** TEM analysis of  $\text{TiO}_2$ , Figure 3f) TEM analysis of  $\text{TiO}_2\text{-SiO}_2$  core shell nano composites

UV-Vis absorption spectra of composite after drying show a good transparency between 400 and 800 nm (Fig.5). Actually, the band edge of bulk anatase is  $\approx 3.2$  eV and is also shown on the same graph. After heat treatment, a small modification was observed, due to the presence of anatase nano crystallites. Indeed, the gel was highly transparent, and any absorbance which appeared at energies below the band gap energy was a result of interference fringes and of the high refraction index of Titania. When Si was present, four additional small peaks were observed in the absorption corresponding to the 3P2, 3P1, 3P0 and 1D2 manifolds as seen in Fig.4. Furthermore, presence of  $\text{SiO}_2$  content results in higher transparency in the visible region, due to the smaller particle size and higher dispersity.



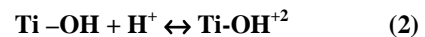
**Fig.5.** UV-Visible spectroscopy of  $\text{TiO}_2$ ,  $\text{TiO}_2\text{-SiO}_2$  nano composites

### 3.1 PHASE ANALYSIS

The gel-derived specimen obtained after being thermally treated at 823 K for 6 h were all non-crystalline as evidenced by XRD analysis. It is known that at about 823 K the equilibrium phase should be cristobalite for  $\text{SiO}_2$  and anatase for  $\text{TiO}_2$ . Accordingly, it is suggested that  $\text{TiO}_2$  and  $\text{SiO}_2$  be mixed uniformly at the atomic scale in the sol-gel conversion may occur simultaneously; however, one of them would be the dominant process at the given conditions. Continuous proceeding of the condensation reaction causes the chain-like structures to have a fast interaction between unreacted OR $\ddot{\text{y}}$  groups and form interchain bonding, which increases the strength of gel structure. Heat treatment will collapse the structures of the resultant cross-linked gels, resulting in the formation of particles with irregular shape, wider particle size distribution and low specific surface area. The monomers obtained interact with each other to establish a three dimensional network structure via condensation and form solids with textures like fragments of monolith. Although heat treatment spheroidize these fragments, the calcined particles give a high specific surface areas, due to residual voids in the network structures. Then, the monomers of  $\text{M}(\text{OH})_z$  react with each other to form particle-like polymers. The specific surface areas of these materials after heat treatment are low since the hydrogen bonding between the particles makes the particles pack more efficiently [19].

### 3.2 FORMING MECHANISM OF STABLE PURE $\text{TiO}_2$ AND $\text{SiO}_2$ -MODIFIED $\text{TiO}_2$ HYDROSOLS

Titania is a Lewis acidic oxide [21]. For pure  $\text{TiO}_2$  hydrosol, in the hydrolysis process,  $\text{Ti}(\text{OH})_4$  was formed after Titanium tetra isopropoxide was hydrolyzed by ethanol and deionised water mixture. In the acid-peptization process, a certain amount of HCl, was added and in the neutralization process, the added  $-\text{OH}$  first neutralized the extensive free  $\text{H}^+$  in the mixture and later attacked  $\text{Ti-OH}^{+2}$ .



The pure  $\text{TiO}_2$  colloid particle can be illustrated as below. For  $\text{SiO}_2$ -modified  $\text{TiO}_2$  hydrosols,  $\text{Ti-O-Si}$  bonds were formed as indicated from FTIR. The model proposed by Tanabe et al. [22] assumes that the doped cation enters the lattice of its host and retains its original coordination number. Since the doped cation is still bonded to the same number of oxygen, even though the oxygen atoms have a new coordination number, a charge imbalance is created. The charge imbalance must be satiated, so Lewis sites and Brönsted sites are formed when the charge imbalance is positive and negative, respectively. The charge imbalance is calculated for each individual bond to the doped cation and multiplied by the number of bonds to the cation.  $\text{SiO}_2$  is tetrahedrally coordinated with each oxygen atom bonded to two silicon atoms.  $\text{TiO}_2$  is octahedrally coordinated with each oxygen atom bonded to three titanium

atoms. Since the radius of  $\text{Si}^{4+}$  is much smaller than that of  $\text{Ti}^{4+}$ , the  $\text{Ti}^{4+}$  could be substituted with  $\text{Si}^{4+}$ , and Ti–O–Si bonds were formed. If a silicon atom enters a Titania lattice, each of its four bonds is now attached to an oxygen having 4/6 anion bond. The charge imbalance is  $4 \times (1 - 4/6) = +4/3$ . Since the imbalance is positive, Lewis sites are formed and more hydroxyl groups would be absorbed on the colloid core of  $\text{TiO}_2\text{-SiO}_2$  [23].

### 3.3 DEGRADATION OF DYES

Fig 6, 7 shows the degradation of Isolan black by  $\text{TiO}_2$ ,  $\text{TiO}_2\text{-SiO}_2$  composites respectively. The UV-Visible spectra of initial solution and product under sunlight for 5 hr reaction over  $\text{TiO}_2$ ,  $\text{TiO}_2\text{-SiO}_2$  samples were recorded to determine how deeply Isolan black was degraded. The primary absorption peaks of the dye solution are shows 575nm in the range of 200-800nm. As the reaction time increases the peaks disappear gradually and the full spectrum pattern changes obviously after 5 hr. At the end of the 5<sup>th</sup> reaction time there is no evident absorption peak observed. It indicates that the main chromophores in the original dye solution are destroyed with photocatalytic reaction and proves that the Isolan black is decomposed in the UV/  $\text{TiO}_2$  and UV/  $\text{TiO}_2\text{-SiO}_2$  system.

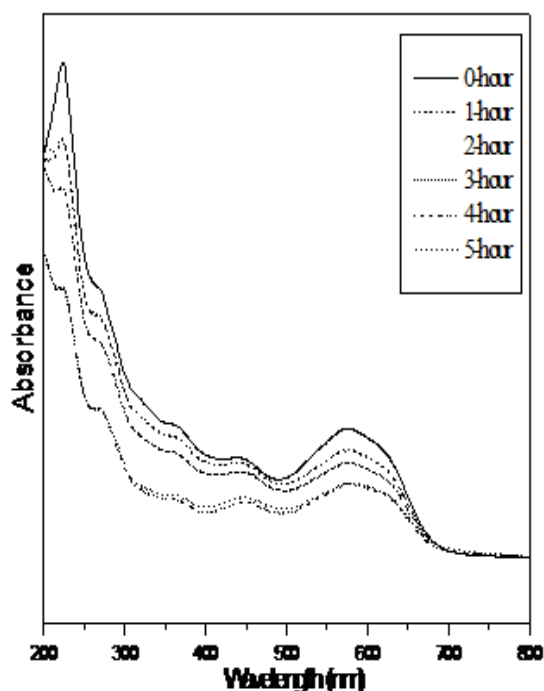


Fig.6. Photo catalytic decomposition of ISOLAN BLACK by  $\text{TiO}_2$ .

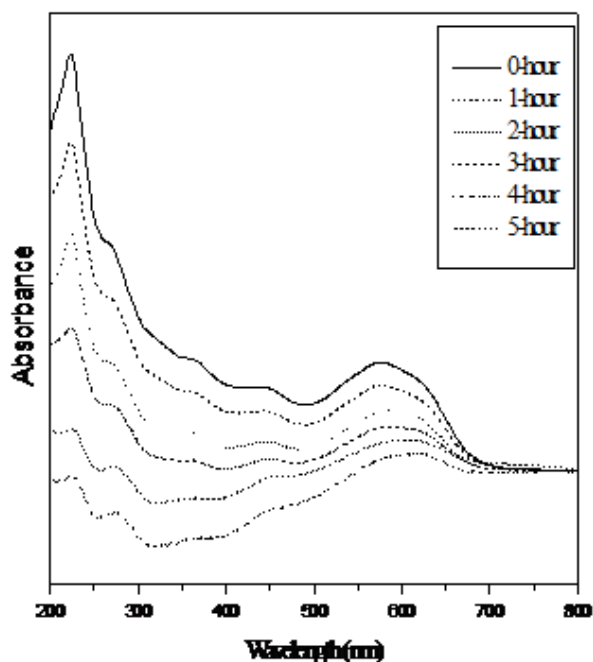


Fig.7. Photo catalytic decomposition of ISOLAN BLACK by  $\text{TiO}_2\text{-SiO}_2$ .

### CONCLUSIONS

$\text{TiO}_2$ ,  $\text{TiO}_2\text{-SiO}_2$  photocatalyst was synthesized by wet chemical method and its photocatalytic activity on degradation of textile dyes were tested. TEM images shows the formation of core shell nano particles. The surface morphology and photocatalytic activity was modified by  $\text{SiO}_2$ . In 5 hour reaction time the concentration level of dye solution lowered down significantly, which indicates  $\text{TiO}_2\text{-SiO}_2$  nanocomposite was effectively degrade the dye molecules.

### REFERENCES

- [1] D. Beydoun, R. Amal, G.Low and S.Mcevoy , Journal of Nanoparticle Research 1, 439-458, 1999.
- [2] Zhang Y., J.C. Crittenden, D.W. Hand & D.L. Perram, a. Fixed-bed photocatalysis for solar decontamination of water. Environmental Science Technology 28: 435–442, 1994
- [3] Hoffmann M.R., S.T. Martin, W. Choi & D. Bahnemann, Environmental applications of semiconductor photocatalysis. Chemical Reviews 95: 69–96, 1995.
- [4] Bahnemann D.W., Ultra small metal oxide particles: Preparation, photophysical characterisation, and photocatalytic properties. Israel Journal of Chemistry 33, 115–136, 1993.

- [5] Julian A. Rengifo-Herrera, Katarzyna Pierzchała, Andrzej Sienkiewicz, Laszlo Forro, John Kiwi, Jacques E. Moser, and Cesar Pulgarin, *J. Phys. Chem. C*, 114, 2717–2723, 2010.
- [6] Yi Xie, Sung Hwan Heo, Seung Hwa Yoo, Ghafar Ali, Sung Oh Cho, *Nanoscale Res Lett* 5:603–607, DOI 10.1007/s11671-009-9513-5, 2010
- [7] Agatino Di Paola, Elisa Garcia-Lopez, Giuseppe Marci, Cristina Martin, Leonardo Palmisano, Vicente Rives, Anna Maria Venezia, *Applied Catalysis B: Environmental* 48, 223–233, 2004.
- [8] Anh Tuan Vu, Quoc Tuan Nguyen, Thi Hai Linh Bui, Manh Cuong Tran, Tuyet Phuong Dang and Thi Kim Hoa Tran, *Adv. Nat. Sci.: Nanosci. Nanotechnol.* 1 015009 (4pp), 2010.
- [9] R.S. Sonawane, B.B. Kale, M.K. Dongare, *Materials Chemistry and Physics* 85 52–57, 2004.
- [10] A. Ennaoui, B.R.Sankapal, V.Skryshevsky, M.Ch.Lux-Steiner, *Solar Energy Materials & Solar Cells* 90 1533–1541, 2006.
- [11] F.Garbassi, L. Balducci, *Microporous and Mesoporous materials* 47, 51-59, 2001.
- [12] Elizabeth Pabon, Jaime Retuert, Raul Quijada, Antonio Zarate, *Microporous and Mesoporous Materials* 67, 195–203, 2004.
- [13] F. Mei, C. Liu, L. Zhang, F. Ren, L.Zhou, W.K.Zhao, Y.L.Fang, *Journal of Crystal Growth* 292 87–91, 2006.
- [14] Jiwei Zhai, Liangying Zhang, Xi Yao *Journal of Non-Crystalline Solids* 260, 160-163, (1999)
- [15] Jose Aguado, Rafael van Grieken, MariaJose Lopez Munoz, Javier Marugan, *Applied Catalysis A: General* 312, 202–212, 2006.
- [16] Hsuan Fu Yu, Shenq Min Wang, *Journal of Non-Crystalline Solids*, 261, 260-267, 2000.
- [17] Zhai Jiwei, Zhang Liangying, Yao Xi, S.N.B. Hodgson, *Surface and Coatings Technology* 138, 135-140, 2001.
- [18] A. Alvarez-Herrero, G. Ramos, F.del Monte, E. Bernabeu, D. Levy, *Thin Solid Films* 455 –456 356–360, 2004.
- [19] A.A. Belheker, S.V. Awate, R. Anand, Photocatalytic, Activity of Titania Modified Mesoporous Silica for Pollution, *Control. Catal. Commun.* 3 pp.453-458, 2002.
- [20] Meihong Zhang, Liyi Shi, Shuai Yuan, Yin Zhao, Jianhui Fang, Synthesis and photocatalytic properties of highly stable and neutral TiO<sub>2</sub>/SiO<sub>2</sub> hydrosol, *J.Colloid and Interface Science*, 330, pp.113–118, 2009.
- [21] P.K. Doolin, S. Alerasool, D.J. Zalewski, J.F. Hoffman, Acidity studies of titania-silica mixed oxides. *Catal. Lett.* 25, pp.209, 1994.
- [22] K. Tanabe, T. Sumiyoshi, K. Shibata, T. Kiyoura, J. Kitagawa, A new hypothesis regarding the surface acidity of binary, metal oxides. *Bull. Chem. Soc. Jpn.*, 47, pp.1064, 1974
- [23] P.P. Yang, Z.W. Quan, C.X. Li, J. Yang, H. Wang, X.M. Liu, J. Lin *J. Solid State Chem.* 181 pp.1943, 2008.